bonding and antibonding carbon valence orbitals. Therefore, one element of the chemical shielding tensor has a much larger paramagnetic contribution than the other two. (3) The dipolar coupling interaction allows not only the assignment of the chemical shielding tensor orientation, but also the determination of local molecular geometry ("nanoscopic MRI").

An extension of this work, NMR sensitivity permitting,[70] is the qualitative prediction and observation of surface-bound species. The detection of bridging methylene units on surfaces has been particularly difficult.[71] Given that various aspects of the problem are already known in some detail, bonding[72] and Knight shift,[73] it should be possible to qualitatively predict some aspects of the chemical shielding tensor for a surface-bound species.

Acknowledgment. The support of the National Science Foundation (Grant CHE-8715517) is gratefully acknowledged. The purchase of the Bruker MSL 200 NMR spectrometer was made possible by NSF Grant CHE-8711788. Useful discussions with R. W. Hall, N. R. Kestner, B. E. Bursten, G. G. Stanley, E. T. Samulski, D. G. Cory, and A. N. Garroway are gratefully acknowledged. L.G.B. is a Fellow of the Alfred P. Sloan Foundation (1989-1991).

Note Added in Proof. A recent compilation by Duncan[74] nicely clarifies the issue of chemical shift scales. To make our labels consistent with Duncan's, change σ to δ except for eq 4.

(69) Collman, J. P.; Hegedus, L. S.; Norton, J. R.; Finke, R. G. *Principles and Applications of Organotransition Metal Chemistry*; University Science Books: Mill Valley, CA, 1987; Table 6.1.
(70) See, for example: Pruski, M.; Kelzenberg, J. C.; Gerstein, B. C.; King, T. S. *J. Am. Chem. Soc.* **1990**, *112*, 4232-40.
(71) Albert, M. R.; Yates, J. T., Jr. *The Surface Scientist's Guide to Organometallic Chemistry*; American Chemical Society: Washington, DC, 1987.
(72) (a) Zheng, C.; Apeloig, Y.; Hoffmann, R. *J. Am. Chem. Soc.* **1988**, *110*, 749-74. (b) Hoffmann, R. *Rev. Mod. Phys.* **1988**, *60*, 601-28.
(73) (a) Wang, P.-K.; Slichter, C. P.; Sinfelt, J. H. *Phys. Rev. Lett.* **1984**, *53*, 82-5. (b) Ansermet, J.-P.; Wang, P.-K.; Slichter, C. P.; Sinfelt, J. H. *Phys. Rev. B* **1988**, *37*, 1417-28.
(74) Duncan, T. M. *A Compilation of Chemical Shift Anisotropies*; Farragut Press: Chicago, 1990.

Determination of Lateral Diffusion Coefficients in Air-Water Monolayers by Fluorescence Quenching Measurements

F. Caruso,[†] F. Grieser,[†] A. Murphy,[†] P. Thistlethwaite,*[,†] R. Urquhart,[†] M. Almgren,[‡] and E. Wistus[‡]

Contribution from the Chemistry School, Melbourne University, Parkville 3052, Australia, and Department of Physical Chemistry, University of Uppsala, S-75121 Uppsala, Sweden.
Received November 19, 1990. Revised Manuscript Received February 11, 1991

Abstract: The fluorescence quenching of a lipoidal pyrene derivative, by two amphiphilic quenchers, at the air-water interface, has been studied by steady-state and time-resolved methods. The results have been analyzed in the theoretical framework of diffusion-controlled quenching in a two-dimensional environment to yield the mutual lateral diffusion coefficients.

Introduction

The biological significance of lateral diffusion of molecules embedded in membranes has led to a number of studies of lateral diffusion in natural membranes and phospholipid bilayers[1-12] and in monolayers.[13-18] The monolayer at the air-water interface is a particularly useful model system in which to study lateral diffusion because of the control that can be exerted over the composition and packing of the monolayer, as well as the nature of the subphase. There has however been some controversy as to how well diffusion in the monolayer models that in the membrane. Early studies of diffusion in monolayers at the air-water interface, using various techniques, yielded values of the diffusion coefficient at least an order of magnitude larger than those reported earlier for lipid bilayers and membranes.[13-15]

There have been a number of approaches to the measurement of lateral diffusion coefficients in monolayers. In what might be termed the "direct" approach, the movement of a probe molecule from one region to another is monitored by some suitable technique. The diffusion coefficient is unambiguously defined in terms of the average distance diffused per unit time. An example of this approach is the fluorescence recovery after photobleaching (FRAP) technique,[1,2,13,18] which involves monitoring the regrowth of fluorescence due to fluorophores diffusing into a pulse photobleached region. While being straightforward in interpretation, the FRAP method faces experimental difficulties related to surface flow, caused by minute temperature gradients at the air-water interface. Such surface streaming can interfere with the diffusion

* To whom correspondence should be addressed.
[†] Melbourne University.
[‡] University of Uppsala.

(1) Peters, R. *Cell Biol. Int. Rep.* **1981**, *5*, 733.
(2) Cherry, R. J. *Biochim. Biophys. Acta* **1979**, *559*, 289.
(3) Edidin, E. In *Membrane Structure*; Finean, J. B., Michell, R. H., Eds.; Elsevier/North-Holland: Amsterdam, 1981.
(4) Wu, E.-S.; Jacobson, K.; Papahajopoulos, D. *Biochemistry* **1977**, *16*, 3936.
(5) Galla, H.-J.; Sackmann, E. *Ber. Bunsen-Ges. Phys. Chem.* **1974**, *78*, 949.
(6) Galla, H.-J.; Sackmann, E. *Biochim. Biophys. Acta* **1974**, *339*, 103.
(7) Kano, K.; Kawazumi, H.; Ogawa, T.; Sunamoto, J. *J. Phys. Chem.* **1981**, *85*, 2204.
(8) Trauble, H.; Sackmann, E. *J. Am. Chem. Soc.* **1972**, *94*, 4499.
(9) Devaux, P.; McConnell, H. M. *J. Am. Chem. Soc.* **1972**, *94*, 4475.
(10) Scandella, C. J.; Devaux, P.; McConnell, H. M. *Proc. Natl. Acad. Sci. U.S.A.* **1972**, *69*, 2056.
(11) Vanderkooi, J. M.; Fischkoff, S.; Andrich, M.; Podo, F.; Owen, C. S. *J. Chem. Phys.* **1975**, *63*, 3661.
(12) Miller, D. D.; Evans, D. F. *J. Phys. Chem.* **1989**, *93*, 323.
(13) Teissié, J.; Tocanne, J.-F.; Baudras, A. *Eur. J. Biochem.* **1978**, *83*, 77.
(14) Loughran, T.; Hatlee, M. D.; Patterson, L. K.; Kozak, J. *J. Chem. Phys.* **1980**, *72*, 5791.
(15) Stroeve, P.; Miller, I. *Biochim. Biophys. Acta* **1975**, *401*, 157.
(16) Subramanian, R.; Patterson, L. K. *J. Am. Chem. Soc.* **1985**, *107*, 5820.
(17) Bohorquez, M.; Patterson, L. K. *J. Phys. Chem.* **1988**, *92*, 1835.
(18) Peters, R.; Beck, K. *Proc. Natl. Acad. Sci. U.S.A.* **1983**, *80*, 7183.

0002-7863/91/1513-4838$02.50/0

due to Brownian motion and can also lead to a lack of definition of the radius of the photobleached area, a quantity that must be known exactly for accurate results.[18]

An alternative strategy is to derive the diffusion coefficient from bimolecular reaction rate data. This approach requires consideration of the particular features of diffusion in two dimensions. The air–water monolayer is an ideal model system for the study of diffusion-controlled reactions in a two-dimensional environment.

The theory of diffusion-controlled reaction in two dimensions has been dealt with by a number of authors.[19-21] It is worth briefly summarizing the differences between diffusion-controlled reaction in a two-dimensional environment and the more familiar three-dimensional case. In three dimensions, following an initial transient period in which the reactivity falls rapidly, a diffusional steady state is established. Except in the case of very viscous solvents, this initial period is very short and can usually be ignored. Once the diffusional steady state is established, the rate of reaction can be written as the product of the (diffusion-controlled) rate constant and the concentrations of the reacting species. In the case of a pseudo-first-order quenching reaction, this is the familiar Stern–Volmer regime. By contrast, in two dimensions, no diffusional steady state is ever attained; the reactivity continues to decline with time, and it is not possible to write the rate of the bimolecular reaction in terms of a time-independent rate constant and reactant concentrations.

Although a number of authors have used bimolecular reaction rate data to study diffusion in two-dimensional or quasi-two-dimensional membrane or micelle environments,[5-7,11-17] there has been a tendency to skirt these difficulties in interpretation. In many cases, approximate methods have been used to extract the diffusion coefficient from reaction rate data.[5,6,17]

The most readily applied theoretical treatment of fluorescence quenching in a two-dimensional environment has been given by Owen.[20] This theory has subsequently been applied to the quenching of pyrene emission in bilayer vesicles, by excimer formation,[11] and by aromatic amine quenchers.[7]

In determinations of the lateral diffusion coefficient based on bimolecular reaction rate data, the most commonly studied reaction has been that of pyrene excimer formation.[5,6,11,17] Notwithstanding the familiarity of this system and the high quantum yield of pyrene (an important consideration in monolayer work), there are disadvantages that relate to the possibility of excimer dissociation complicating the kinetics.[22] The conformational requirements for excimer formation also raise the question of whether purely translational diffusion is being observed. From this point of view, an irreversible fluorescence quenching reaction is to be preferred as the basis of a lateral diffusion study.

The air–water monolayer has certain advantages over the bilayer vesicle as a model system for the study of two-dimensional quenching: it is a strictly two-dimensional system and, moreover, readily permits the study of the effect of surface pressure. The work to be described in this paper had two aims. First, we were concerned to see to what extent features predicted to be peculiar to two-dimensional quenching were evident in the data, and second, we wished to check the agreement between diffusion coefficients extracted from bimolecular quenching data and those obtained from the best FRAP experiments. The present study deals mainly with steady-state fluorescence quenching of *N*-(1-pyrenylsulfonyl)dipalmitoyl-L-α-phosphatidylethanolamine (pyrene-DPPE), by octadecyldimethylamine (ODMA), and 4-(dimethylhexadecylammonio)-2,2,6,6-tetramethylpiperidine-1-oxyl iodide (CAT-16), in dioleoyl-L-α-phosphatidylcholine (DOPC) monolayers, over an extended surface pressure range. Time-resolved measurements were also made. Values of the mutual lateral diffusion coefficient were derived by using the formalism developed by Owen. Pyrene-DPPE is in some ways an ideal amphiphile for the present sort of study: the fluorescence quantum yield is high, and unlike the case of many long-chain pyrene derivatives, there is little tendency to form excimers at moderate dilution in DOPC monolayers. In another respect, to be discussed at a later point, pyrene-DPPE is less than ideal.

(19) Razi Naqvi, K. *Chem. Phys. Lett.* **1974**, *28*, 280.
(20) Owen, C. S. *J. Chem. Phys.* **1975**, *62*, 3204.
(21) Torney, D. C.; McConnell, H. M. *Proc. R. Soc. London, A* **1983**, *387*, 147.
(22) Alsins, J.; Almgren, M. *J. Phys. Chem.*, in press.

Experimental Details

Pyrene-DPPE and CAT-16 were obtained from Molecular Probes Inc. ODMA was purchased from Pfaltz and Bauer Inc., and DOPC from Sigma Chemical Co. All were used without further purification. All nonaqueous solvents were spectroscopic grade. Water used in all experiments was obtained from a Milli-Q system ($\kappa < 1 \times 10^{-6}\ \Omega^{-1}\ cm^{-1}$, surface tension ($\gamma_0$) = 72 mN m^{-1} at 25 °C).

All glassware was soaked in hot alkaline detergent for 2 h, rinsed thoroughly with deionized water and Milli-Q water, and then soaked in hot nitric acid for at least 1 h. Following this, the glassware was rinsed with Milli-Q water, steam-cleaned for at least 30 min, further rinsed with Milli-Q water and methanol, and finally dried at 100 °C. Between experiments, the Langmuir trough was cleaned with the spreading solvent and was periodically cleaned with hexane, methanol, and chloroform to remove any possible contaminants.

Solution fluorescence experiments were performed on a Perkin-Elmer LS-5B spectrofluorimeter, and solution absorption experiments on a data processor controlled Hitachi 150-20 spectrophotometer. Surface pressure–area measurements for the pure amphiphile monolayers were conducted on a 57.9 × 13.5 cm^2 PTFE Langmuir trough, with a solid PTFE barrier, driven at a compression rate of 0.03 nm^2 $molecule^{-1}$ min^{-1}. A 59.7 × 16.5 cm^2 PTFE Langmuir trough, with a barrier speed of 0.05 nm^2 $molecule^{-1}$ min^{-1}, was used for monolayers containing more than one type of amphiphile and for steady-state fluorescence measurements. The surface pressure–area isotherms for these mixed monolayers were recorded while the fluorescence measurements were performed. In both cases, the surface pressure was measured by the Wilhelmy hanging plate method, using a 4.3 cm wide mica plate suspended from a Shinkoh 2-g-capacity strain gauge. As the monolayer was compressed, the apparent changes in weight of the mica plate were converted to voltages by the strain gauge and displayed on a Curkin chart recorder. The mica plate was roughened and was periodically cleaned with AR nitric acid, followed by thorough rinsing with Milli-Q water, to ensure a zero degree contact angle with water. Experiments were initiated by filling the trough with the appropriate subphase, which was either an aqueous solution of 0.1 M $NaClO_4$ or an aqueous solution of 0.1 M $NaClO_4$ containing 0.03 M NaOH. The spreading solvent used for all monolayer experiments was chloroform. Approximately 10^{17} molecules were spread dropwise onto the subphase by using a 100-μL glass syringe. The solvent was then allowed to evaporate for 10 min, after which the monolayer was compressed as desired.

Steady-state fluorescence measurements were recorded on a Perkin-Elmer LS-5 spectrofluorimeter. Two optical fiber bundles (excitation fiber, Dyonics; emission fiber, Dolan Jenner), terminating approximately 5 mm above the monolayer, were used to convey the exciting light and the fluorescence to and from the monolayer. A neutral-density filter was placed on the bottom of the trough to minimize scatter and reflection of the exciting light. The trough was kept in darkness during the experiments. The fluorescence spectrum of the monolayer was obtained by separately scanning the "background spectrum" in the absence of the monolayer and the "total spectrum" in the presence of the monolayer and then subtracting. Fluorescence spectra were signal-averaged over 25 scans to increase the signal-to-noise ratio.

The pyrene-DPPE fluorescence maximum is at a wavelength of 380 nm. The background scattered from the subphase was monitored for 20 min at 380 nm, taking readings every 1 s to increase the signal-to-noise ratio. The average value over this period was used as the blank. The monolayer was spread, and the solvent was allowed to evaporate. The monolayer was then compressed while both the fluorescence intensity at 380 nm and the surface pressure–area isotherm of the monolayer were recorded. The blank was then subtracted in order to obtain the fluorescence intensity variation with surface pressure and area per molecule (Figure 1). Thus the fluorescence intensities at various surface pressures (I values) were obtained for each of the monolayers of different quencher concentration. The I_0 value at a given surface pressure was obtained from a monolayer containing only pyrene-DPPE in DOPC (reference system). As the pyrene-DPPE fluorescence lifetime was found to be surface pressure dependent (see later), it was necessary to apply a correction in the following manner. Due to the difference in composition between the monolayers with quencher and the reference system, at any given surface pressure, the area per pyrene-DPPE in the reference system will differ from that in any of the films with quencher. Accordingly, the intensity from the reference system at a given surface pressure was corrected by multiplying by the ratio of the pyrene-DPPE surface densities in the system under consideration and the reference. All

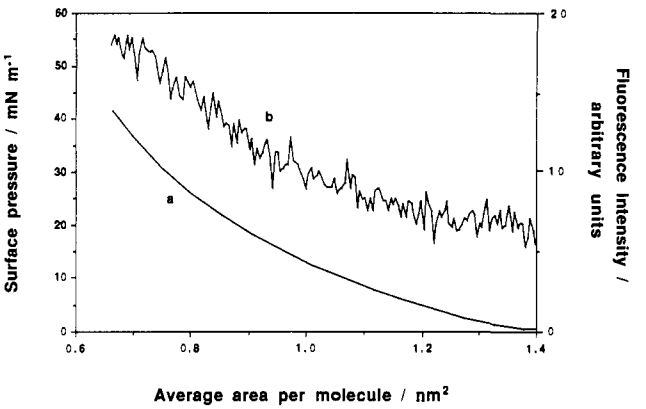

Figure 1. Surface pressure–area isotherm and fluorescence intensity versus area per molecule curve of a 1 mol % pyrene-DPPE/99 mol % DOPC monolayer: (a) surface pressure–area isotherm; (b) fluorescence intensity of pyrene-DPPE as the monolayer was compressed, λ_{ex} = 327 nm and λ_{em} = 380 nm. Temperature = 20 ± 1 °C.

monolayer fluorescence measurements were made with the monolayer and subphase air-equilibrated. The fluorescence lifetime of pyrene-DPPE was found to be sufficiently short so as to rule out the possibility of oxygen quenching.

Fluorescence decay times were measured by the time-correlated single-photon-counting method on two different systems. Values of the fluorescence lifetime of pyrene-DPPE in solution were measured on a synchronously Ar^+-laser-pumped, mode-locked, cavity-dumped Rh 6G dye laser, at Melbourne University. Monolayer decay time measurements were made on a Nd:YAG-pumped dye laser at the Department of Physical Chemistry, University of Uppsala. The frequency-doubled output of the YAG laser was used to synchronously pump a Rh 6G dye laser. The mode-locked, cavity-dumped output of this laser was then frequency-doubled to give 320-nm radiation. The exciting light was focused onto the water surface of a 44.2 × 15.0 cm^2 PTFE Langmuir trough by means of a lens and mirror. The exciting beam then passed through a silica window mounted in the bottom of the trough and into a black box, which acted as a light sink, reducing the intensity of scattered exciting light. The monolayer fluorescence was detected by a Hamamatsu microchannel-plate photomultiplier tube (R15640). The monolayer fluorescence was focused onto the phototube by a silica lens, with the wavelength of observation (400 nm) determined by an Oriel narrow-band interference filter. Lifetime measurements were made more difficult by the occurrence of a time-dependent "background" signal probably due to PTFE fluorescence from the trough. This background was first recorded with a blank water surface. The decay curve of the monolayer was then recorded, and the background was subtracted to give the true decay curve. With this procedure, it is imperative that the sample and background decay curves be collected for the same total excitation intensity. This was achieved by the use of a diode to monitor the excitation intensity. This diode was connected to a voltage/frequency converter and counter that gated the detection system to operate to a predetermined number of excitation counts. Collection times were typically 20 min, with a cavity-dump frequency of 400 kHz and average UV power of 50 μW.

Results

Solution Quenching Measurements. Prelinary experiments were conducted to verify that quenching of pyrene-DPPE by ODMA and CAT-16 is diffusion-controlled in bulk solution. The second-order quenching rate constants extracted from these data were 8.5 × 10^8 and 5.5 × 10^9 M^{-1} s^{-1} for ODMA and CAT-16, respectively, on the basis of an unquenched fluorescence lifetime of pyrene-DPPE in methanol of 13.2 ns. In the CAT-16 case, the correction procedure of Demas and Adamson was used.[23] The value of 8.5 × 10^8 M^{-1} s^{-1} found for ODMA is somewhat below that estimated from the Debye–Smoluchowski equation (ca. 6 × 10^9 M^{-1} s^{-1}) and suggests that there is a small activation barrier to quenching. In the case of CAT-16, the data are in accord with an earlier report that CAT-16 quenches the fluorescence of aromatic hydrocarbons at a diffusion-controlled rate.[24]

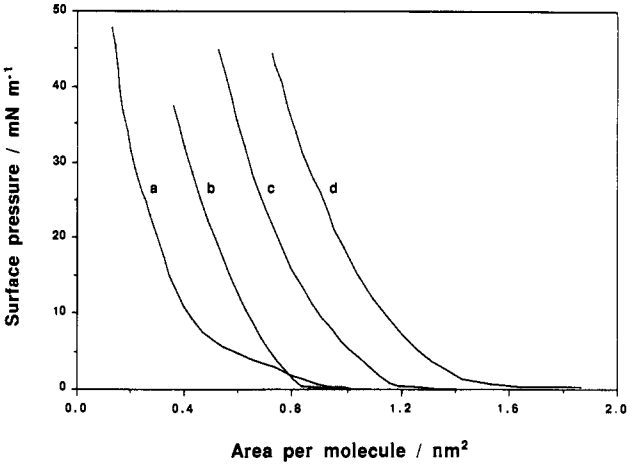

Figure 2. Surface pressure–area isotherms of the pure amphiphile monolayers: (a) ODMA; (b) CAT-16; (c) DOPC; (d) pyrene-DPPE. All isotherms were recorded at 19 ± 1 °C.

Surface Pressure–Area Isotherms. Surface pressure–area isotherms for the various amphiphiles, by themselves and in combination with each other, were measured in order to confirm the stability of the amphiphiles at the interface and to determine limiting molecular cross-sectional areas for the later determination of interaction radii. Results for the pure amphiphile monolayers are shown in Figure 2. For ODMA it was found that surface pressure stability at the air–water interface could only be obtained by incorporatintg 0.1 M $NaClO_4$ in the subphase. With a pH of 12.5 (to prevent protonation of the amino group and consequent loss of quenching capacity), the limiting area per molecule was found to be 0.30 nm^2. The "expanded" type isotherm showed no discontinuities suggestive of phase changes. On the same subphase DOPC and pyrene-DPPE showed "expanded" isotherms with limiting areas of 0.83 and 1.10 nm^2, respectively. The former is in good agreement with literature values,[17,25] while the latter value agrees well with the value reported for the related molecule 1-(6-pyrenylhexanoyl)-2-palmitoyl-*sn*-glycero-3-phosphocholine.[17] For CAT-16 on a 0.1 M $NaClO_4$ subphase an "expanded" isotherm was obtained that yielded a limiting area of 0.65 nm^2. The surface pressure–area isotherms for both DOPC and pyrene-DPPE on a 0.1 M $NaClO_4$ subphase were found to be identical with those for spreading on a basic 0.1 M $NaClO_4$ subphase. Isotherms for monolayers containing 1 mol % pyrene-DPPE (the amount needed for good signal-to-noise ratio in the fluorescence measurements) with various amounts of ODMA or CAT-16, diluted in DOPC, on subphases of 0.1 M $NaClO_4$ or 0.1 M $NaClO_4$ plus 0.03 M NaOH, respectively, were also recorded. In both cases, the isotherms showed the monolayers to be in the "expanded" state throughout, with there being no evidence of phase transitions or immiscibility of components. As expected, the isotherms moved to lower average areas per molecule with increase in the mole fraction of the smaller ODMA or CAT-16.

Monolayer Spectra. The excitation (emission 400 nm) and emission (excitation 327 nm) spectra of a 1 mol % pyrene-DPPE in DOPC monolayer were recorded. No excimer emission could be detected. Moreover, the monomer emission intensity was constant over time. Similarly, the fluorescence intensity of the monolayers containing both pyrene-DPPE and ODMA or CAT-16 diluted in DOPC showed constant emission intensity. As we have previously reported,[26] such observations provide evidence for homogeneity and miscibility of components.

Steady-State Quenching Measurements. Stern–Volmer plots for the quenching of 1 mol % pyrene-DPPE diluted in DOPC, by ODMA, at various surface pressures, are shown in Figure 3. In each case the subphase was 0.1 M $NaClO_4$ at pH 12.5. The

(23) Demas, J. N.; Adamson, A. W. *J. Am. Chem. Soc.* **1973**, *95*, 5159.
(24) Green, J. A.; Singer, L. A. *J. Chem. Phys.* **1973**, *58*, 2690.
(25) Tancrède, P.; Parent, L.; Paquin, P.; Leblanc, R. *J. Colloid Interface Sci.* **1981**, *83*, 606.
(26) Urquhart, R. S.; Hall, R. A.; Thistlethwaite, P. J.; Grieser, F. *J. Phys. Chem.* **1990**, *94*, 4173.

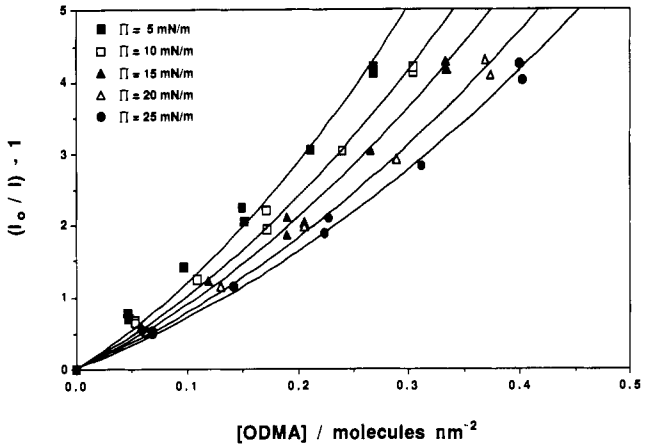

Figure 3. Stern–Volmer plots for the quenching of 1 mol % pyrene-DPPE by ODMA in DOPC monolayers at various surface pressures. Subphase: 0.1 M $NaClO_4$ plus 0.03 M NaOH. λ_{ex} = 327 nm and λ_{em} = 380 nm. Temperature = 19 ± 1 °C. The solid lines are theoretical curves calculated by using eq 2, with parameters given in the text.

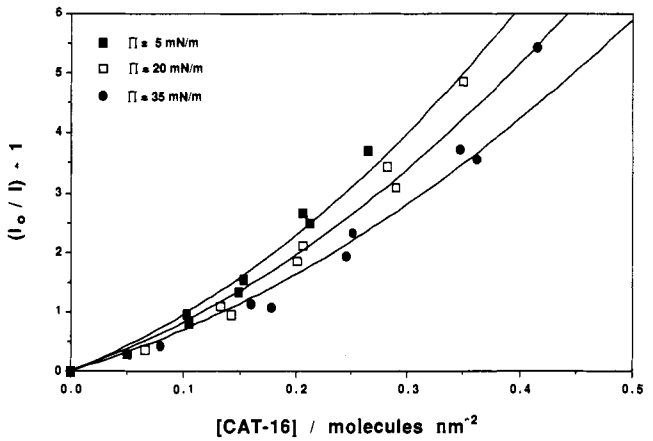

Figure 4. Stern–Volmer plots for the quenching of 1 mol % pyrene-DPPE by CAT-16 in DOPC monolayers at various surface pressures. Subphase: 0.1 M $NaClO_4$, λ_{ex} = 327 nm and λ_{em} = 380 nm. Temperature = 21 ± 2 °C. The solid lines are theoretical curves calculated by using eq 2, with parameters given in the text.

plots show the expected upward curvature characteristic of quenching in a two-dimensional environment.[7] Corresponding plots for the quenching by CAT-16 are given in Figure 4.

Owen has derived an equation for the time dependence of the fluorescence intensity in the presence of two-dimensional quenching. The time dependence can be expressed as

$$I(t)/I_0 = \exp\{-t/\tau_0 - 7.44[Q]R(tD)^{1/2} - 2.28[Q]Dt\} \quad (1)$$

where τ_0 is the unquenched fluorescence lifetime, [Q] the quencher concentration expressed as molecules per unit area, D the lateral diffusion coefficient, and R the interaction distance, defined as the distance of closest approach of the fluorophore and quencher. Derivation of the above approximate equation involves replacing an integral with an empirical function that provides a good approximation to the integral for $t < 5R^2/D$. A recalculation of this integral in the appropriate time range leads to the numerical constants in the above expression having values slightly different from those given by Owen. We are indebted to Bo Medhage of the Department of Physical Chemistry, University of Uppsala, for this calculation.

The equation for the time dependence of the fluorescence can be integrated to give the steady-state quenching equation

$$I/I_0 = (a\tau_0)^{-1}\{1 - b(\pi/a)^{1/2}[\exp(b^2/a)]\ \mathrm{erfc}\ (b^2/a)^{1/2}\} \quad (2)$$

where $a = \tau_0^{-1} + 2.28D[Q]$ and $b = 3.72D^{1/2}R[Q]$. The function erfc (x) is the complementary error function as defined in standard

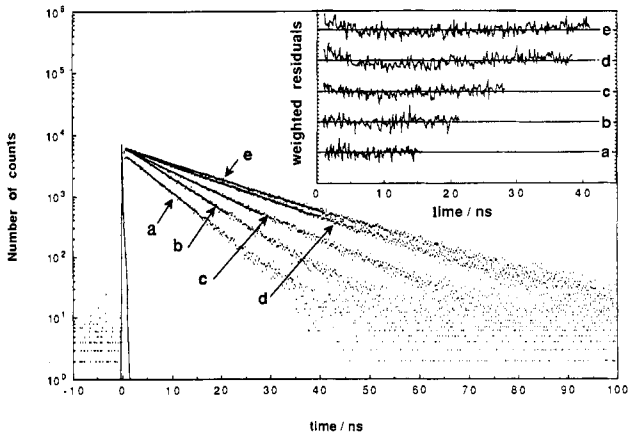

Figure 5. Fluorescence decays of a 1 mol % pyrene-DPPE/99 mol % DOPC monolayer at various surface pressures: (a) π = 5 mN m^{-1}; (b) π = 10 mN m^{-1}; (c) π = 20 mN m^{-1}; (d) π = 30 mN m^{-1}; (e) π = 35 mN m^{-1}. Subphase: 0.1 M $NaClO_4$. λ_{ex} = 320 nm and λ_{em} = 400 nm. Temperature = 23 ± 0.5 °C. The inset shows the weighted residuals from single-exponential fits to each of the curves; one unit on the weighted residuals axis equals 1 standard deviation.

Table I. Mutual Diffusion Coefficients for Pyrene-DPPE with ODMA or CAT-16 in DOPC Monolayers, Obtained by Steady-State and Time-Resolved Methods

		D, $cm^2\ s^{-1} \times 10^7$			
		steady-state		time-resolved	
π, mN m^{-1}	τ_0(py-DPPE), ns	ODMA	CAT-16	CAT-16 (10%)	CAT-16 (20%)
5	6.6	21.2	11.9	6.3	5.3
10	8.2	13.7	8.8	5.1	4.1
15		9.8	6.8		
20	11.1	7.2	5.8	3.3	3.1
25		5.3	4.8		
30	14.8		3.8	2.9	2.2
35	16.3		3.1	2.1	1.8

tables. The data of Figures 3 and 4 were least-squares-fitted to eq 2. The least-squares fit requires values for R and τ_0. Interaction distances were calculated as the sum of the molecular radii, in turn calculated from the limiting molecular cross-sectional areas obtained from the surface pressure–area isotherms. Interaction distances for pyrene-DPPE with ODMA and CAT-16 were calculated to be 0.8 and 1.0 nm, respectively. The expanded nature of the CAT-16 and pyrene-DPPE monolayers introduces some uncertainty into the determination of the interaction distances.

Time-Resolved Quenching Measurements. Fluorescence decay times for 1 mol % pyrene-DPPE diluted in DOPC were measured over the range of surface pressure covered by the steady-state quenching measurements. The results are shown in Figure 5. The single-exponential fluorescence decay behavior confirms that pyrene-DPPE is not aggregated in the monolayer film. The decay time increased from a value of 6.6 ns at 5 mN m^{-1} to 16.3 ns at 35 mN m^{-1}. These lifetimes were used in fitting the data of Figures 3 and 4 and are given in Table I. The increase in lifetime of pyrene-DPPE with increase in surface pressure is most plausibly attributable to the decline in the effective polarity of the environment as the DOPC monolayer is compressed.[27]

Time-resolved measurements were performed on the CAT-16/pyrene-DPPE system to check their consistency with the steady-state data. Measurements were made for 10 and 20 mol % CAT-16, for surface pressures ranging from 5 to 35 mN m^{-1}. As expected from the Owen analysis of two-dimensional diffusion, the decays were clearly nonexponential. Typical decay curves are shown in Figure 6. The decay curves were least-squares-fitted to the time dependence equation (1), by using a value of 1.0 nm

(27) Grieser, F.; Thistlethwaite, P.; Urquhart, R.; Patterson, L. K. *J. Phys. Chem.* **1987**, *91*, 5286.

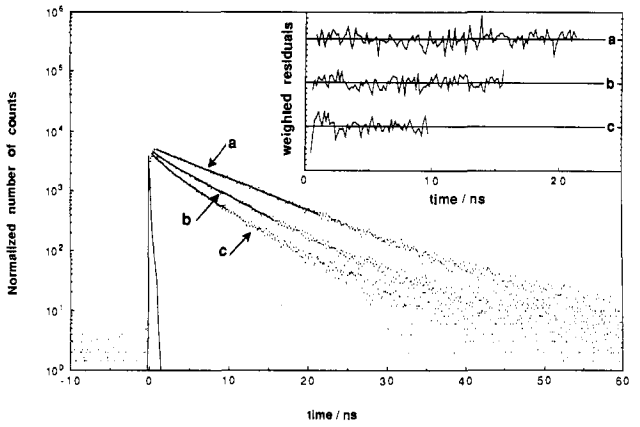

Figure 6. Fluorescence decays of a 1 mol % pyrene-DPPE/CAT-16/DOPC monolayer for various concentrations of CAT-16 at π = 10 mN m^{-1}: (a) 0 mol % CAT-16; (b) 10 mol % CAT-16; (c) 20 mol % CAT-16. All intensities normalized to the same fitted value at t = 0. Subphase: 0.1 M $NaClO_4$. λ_{ex} = 320 nm and λ_{em} = 400 nm. Temperature = 23 ± 0.5 °C. The inset shows the weighted residuals from a single-exponential fit to curve a and the fits to the Owen equation for curves b and c; one unit on the weighted residuals axis equals 1 standard deviation.

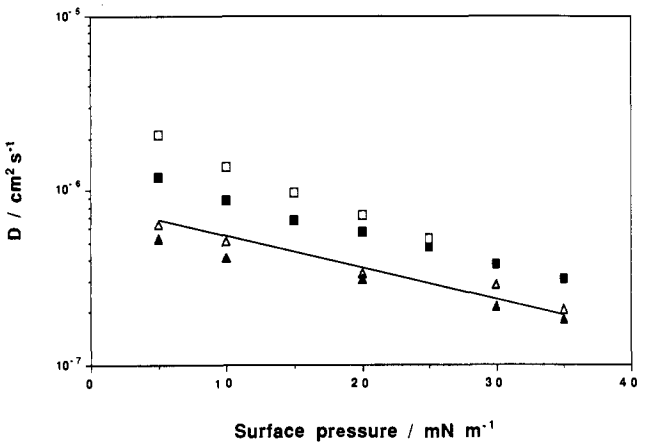

Figure 7. Logarithm of the lateral diffusion coefficients versus surface pressure for pyrene-DPPE with ODMA or CAT-16 in DOPC monolayers, obtained by using steady-state and time-resolved methods. Steady-state: (□) ODMA; (■) CAT-16. Time-resolved: (△) 10 mol % CAT-16; (▲) 20 mol % CAT-16. The solid line is a linear fit to the data of Peters and Beck for the diffusion of *N*-[4-nitrobenz-2,1,3-oxadiazole] egg phosphatidylethanolamine in L-α-dilauroylphosphatidylcholine monolayers, obtained by using the FRAP technique.

for the interaction distance. The results of this fitting are shown in Table I.

Discussion

The D values collected in Table I show the expected trend of increase with fall in surface pressure. The log of the D value varies approximately linearly with the surface pressure (Figure 7). A similar trend has been reported by Peters and Beck[18] in a study of diffusion in L-α-dilauroylphosphatidylcholine monolayers using the FRAP technique. The D values obtained from the steady-state measurements are larger than those obtained from the time-resolved data, while the ODMA steady-state data yield higher D values than do those for CAT-16. The comparison of the ODMA and CAT-16 steady-state data is particularly significant. The bulk solution quenching results might have suggested a tendency for the ODMA data to underestimate the diffusion coefficient. The higher values obtained for the latter case support the view that essentially the same diffusional process is monitored in both cases and that the larger D values found for the ODMA experiments reflect the smaller size of ODMA compared to CAT-16. It should be noted that whereas in the FRAP study of Peters and Beck it is the diffusion coefficient of the fluorescent lipid that is measured, in this case it is the mutual diffusion coefficient of pyrene-DPPE and the quencher in question.

For the steady-state measurements, the quencher concentration ranges from a low of 5 mol % to a high of 25 mol %. Clearly, at the highest quencher concentration, diffusion is occurring in a monolayer that is substantially different from that in which the quencher concentration is low. Indeed, at the highest quencher concentration, the calculated average quencher–fluorophore distance is virtually equal to the interaction distance. Despite this, the fit of the I_0/I data for ODMA is reasonable over the whole range of quencher concentrations, for all the surface pressures studied. In the CAT-16 case, the experimental values of I_0/I for the highest quencher concentration always lie above the curves fitted to the other points. For this reason, the 25 mol % quencher data were omitted from the fits. The above considerations, and the fact that the steady-state data give higher D values than do the time-resolved, suggest the possibility of static quenching affecting the former. Static quenching might be expected to be most in evidence at high surface pressures, where diffusion is minimal, causing D values for high surface pressures to deviate from the trend of other data. The difference between the D values determined from steady-state and time-resolved data is however greatest at low surface pressures. Moreover, the D values found for high surface pressures fall on the same smooth curve as the data for lower surface pressure.

Notwithstanding the foregoing arguments, static quenching is the most obvious explanation for the divergence of our steady-state and time-resolved data. It is possible that static quenching distorts all the steady-state data (with the effect being greatest at the highest quencher concentrations) and leads to the extraction of high D values. If the probability of fluorophore/quencher pairs decreases at high surface pressure, other things being equal, this could explain the divergence of the steady-state and time-resolved data at low surface pressures. An alternative argument focuses on the surface pressure dependence of the pyrene-DPPE lifetime. The fall in lifetime of pyrene-DPPE with fall in surface pressure means that it is less susceptible to dynamic quenching, for a given D value, at low surface pressure. This in turn suggests that any interference by static quenching will be more apparent at low pressures. We are not at present able to comment further on these possibilities.

The foregoing discussion highlights a problem with the use of pyrene-DPPE in a study of this sort. The short lifetime of pyrene-DPPE necessitates the use of large quencher concentrations if diffusional quenching is to compete with normal decay. Lower quencher concentrations would be possible if a quenchable, amphiphilic fluorophore of longer lifetime were available. On the other hand, such a fluorophore might pose the problem of excluding air from the system, should oxygen quenching prove to be appreciable and not constant with surface pressure.

As mentioned earlier, the uncertainty as to the interaction distance introduces an uncertainty into the calculated D values. For example, in the case of quenching by CAT-16, a change in R from 1.0 to 0.9 nm changes the D values by about 20%. The value of 1.0 nm is our best estimate from the measured limiting molecular areas. Atik and Singer[28] have attempted to work back from measured bulk solution quenching rates to the interaction distance, using known values of solvent viscosity, and have obtained a value of ca. 0.7 nm for the interaction distance for pyrene and 4-(trimethylammonio)-2,2,6,6-tetramethylpiperidine-1-oxyl iodide (CAT-1). It is reasonable that our value for the monolayer should be larger than this. The bulk solution value of R would be expected to reflect the average of all possible relative orientations of the reacting species and could well be less than the value in the monolayer, where some conformational restrictions are expected to apply.

Our time-resolved results for the pyrene-DPPE/CAT-16 system agree well with the FRAP data of Peters and Beck[18] for the diffusion of *N*-[4-nitrobenz-2,1,3-oxadiazole] egg phosphatidylethanolamine (NBD-egg lipid) in L-α-dilauroylphosphatidyl-

(28) Atik, S.; Singer, L. A. *J. Am. Chem. Soc.* **1978**, *100*, 3234.

choline. They agree moderately well with the results of Bohorquez and Patterson for diffusion in DOPC[17] and are somewhat larger than the values obtained earlier by Subramanian and Patterson.[16] Alsins and Almgren[22] have noted that, in measurements based on the pyrene excimer system, neglect of excimer dissociation leads to low D values. This could in part account for the lower results of Subramanian and Patterson. Almgren et al.[29] have also noted that use of the three-dimensional analysis in a two-dimensional situation likewise underestimates D. In their pyrene excimer based study, Bohorquez and Patterson made use of the "semiempirical" relation $D = k/4$, originally introduced by Galla and Sackmann,[5] where k is a quasi-second-order rate constant "forced" on the data. Our analysis of this procedure leads us to conclude that this approach is also likely to lead to a low value of D.

(29) Almgren, M. In *Kinetics and Catalysis in Microheterogeneous Systems*; Kalyanasundaram, K., Grätzel, M., Eds.; Surfactant Science Series; Marcel Dekker: New York, 1991.

Conclusion

Derivation of lateral diffusion coefficients from bimolecular quenching data obtained for an air-water monolayer leads to values comparable to those obtained by the direct, FRAP method. Both the steady-state and time-resolved data show clear evidence for the features predicted for diffusion-controlled reaction in a two-dimensional environment.

Acknowledgment. F.G. and P.T. gratefully acknowledge financial support from the Australian Research Council.

Encapsulated Alkaline-Earth Metallocenes. Synthesis, Solution Behavior, and Solid-State Structures of Bis(tetraisopropylcyclopentadienyl)calcium and -barium, $[(C_3H_7)_4C_5H]_2Ca$ and $[(C_3H_7)_4C_5H]_2Ba$

R. Allen Williams, Kris F. Tesh, and Timothy P. Hanusa*

Contribution from the Department of Chemistry, Vanderbilt University, Nashville, Tennessee 37235. *Received August 29, 1990*

Abstract: Reaction of 2 equiv of KCp^{4i} ($Cp^{4i} = (C_3H_7)_4C_5H$) with CaI_2 in diethyl ether or BaI_2 in THF produces the metallocenes $(Cp^{4i})_2Ca$ and $(Cp^{4i})_2Ba$ in 77 and 83% yields, respectively. The calcium metallocene $(Cp^{4i})_2Ca$ displays a remarkable degree of air stability and can be handled in dry air for several minutes without decomposition. It displays virtually no tendency to form adducts in solution with ethers or aromatic amines. The barium metallocene is the most volatile known organobarium compound, subliming at 90 °C and 0.01 Torr. These physical properties of the metallocenes are most likely related to the ability of the isopropyl groups of the Cp^{4i} rings to interlock, forming "cages" around the metal centers. DNMR experiments have provided evidence for hindered rotation in the complexes, either around the ring-C-$CHMe_2$ bonds or around the metal-ring centroid axis, with energies of activation of $\Delta G^{\ddagger} \leq 11.1$ kcal mol^{-1} in $(Cp^{4i})_2Ca$ and 11.1 (±0.5) kcal mol^{-1} in $(Cp^{4i})_2Ba$. Conformations of the Cp^{4i} anions were probed with semiempirical MO (AM1) calculations and found to be consistent with the solid-state structures. Crystals of $(Cp^{4i})_2Ca$ grown from hexane are monoclinic, space group $C2/c$, with $a = 34.033$ (6) Å, $b = 12.432$ (6) Å, $c = 16.495$ (5) Å, $\beta = 111.29$ (2)°, and $D_c = 1.036$ g cm^{-3} for $Z = 8$. Least-squares refinement on the basis of 2102 observed reflections measured at 23 °C led to a final R value of 0.044. The average Ca-C distance is 2.64 (1) Å, and the ring centroid-Ca-ring centroid angle is 162°. Crystals of $(Cp^{4i})_2Ba$ grown from hexane are triclinic, space group $P\bar{1}$, with $a = 16.682$ (4) Å, $b = 17.862$ (2) Å, $c = 12.396$ (4) Å, $\alpha = 108.02$ (3)°, $\beta = 90.56$ (3)°, $\gamma = 111.12$ (2)°, and $D_c = 1.236$ g cm^{-3} for $Z = 4$. Least-squares refinement on the basis of 6021 observed reflections measured at −120 °C led to a final R value of 0.039. Two crystallographically independent but nearly identical molecules occur in the unit cell. The average Ba-C distance is 2.94 (2) Å, and the ring centroid-Ba-ring centroid angle is 154°.

Introduction

The extent to which coordinated ligands can influence the chemistry of main-group organometallic compounds has traditionally been considered fairly limited.[1] Most main-group metals, for example, have only one or two accessible oxidation states, which restricts the stoichiometry of possible compounds. In addition, the highly ionic bonding associated with the electropositive early main-group elements (groups 1 and 2) frequently lowers the solubility and volatility of their complexes.

Recent developments in early-main-group chemistry have seen some of these limitations narrowed. In particular, the organometallic chemistry of calcium, strontium, and barium has undergone considerable expansion in the last several years as the special ligand requirements for stabilizing these large, electropositive metals have become recognized.[2] Many of the current developments have used the pentamethylcyclopentadienyl ligand (Cp*) as a sterically bulky, stabilizing group, which has lead to complexes with greatly increased solubility in nonpolar media, lower metal coordination numbers, and improved volatility.[3-7] These complexes are perhaps even more sensitive to air and moisture than are their cyclopentadienyl counterparts, however, and they rapidly form adducts with a wide range of Lewis bases, including ethers, aromatic amines, phosphines, isonitriles,[3] and unsaturated hydrocarbons.[8]

(1) Elschenbroich, C.; Salzer, A. *Organometallics: A Concise Introduction*, 1st ed.; VCH Publishers: New York, 1989.

(2) Hanusa, T. P. *Polyhedron* **1990**, *9*, 1345-1362.
(3) Burns, C. J.; Andersen, R. A. *J. Organomet. Chem.* **1987**, *325*, 31-37.
(4) McCormick, M. J.; Williams, R. A.; Levine, L. J.; Hanusa, T. P. *Polyhedron* **1988**, *7*, 725-730.
(5) Williams, R. A.; Hanusa, T. P.; Huffman, J. C. *J. Chem. Soc., Chem. Commun.* **1988**, 1045-1046.
(6) McCormick, M. J.; Sockwell, S. C.; Davies, C. E. H.; Hanusa, T. P.; Huffman, J. C. *Organometallics* **1989**, *8*, 2044-2049.
(7) Williams, R. A.; Hanusa, T. P.; Huffman, J. C. *Organometallics* **1990**, *9*, 1128-1134.

0002-7863/91/1513-4843$02.50/0